



Contents lists available at ScienceDirect

Building and Environment

journal homepage: www.elsevier.com/locate/buildenv

Swimming pools as heat sinks for air conditioners: Model design and experimental validation for natural thermal behavior of the pool

Jonathan Woolley¹, Curtis Harrington*, Mark Modera²

University of California Davis, Western Cooling Efficiency Center, 1450 Drew Avenue, Suite 100, Davis, CA 95618, United States

ARTICLE INFO

Article history:

Received 5 April 2010

Received in revised form

28 June 2010

Accepted 15 July 2010

Keywords:

Swimming pool

Heat sink

Energy efficient air conditioning

Heat transfer model

Experimental validation

Free surface evaporation

ABSTRACT

Swimming pools as thermal sinks for air conditioners could save approximately 40% on peak cooling power and 30% of overall cooling energy, compared to standard residential air conditioning. Heat dissipation from pools in semi-arid climates with large diurnal temperature shifts is such that pool heating and space cooling may occur concurrently; in which case heat rejected from cooling equipment could directly displace pool heating energy, while also improving space cooling efficiency. The performance of such a system relies on the natural temperature regulation of swimming pools governed by evaporative and convective heat exchange with the air, radiative heat exchange with the sky, and conductive heat exchange with the ground. This paper describes and validates a model that uses meteorological data to accurately predict the hourly temperature of a swimming pool to within 1.1 °C maximum error over the period of observation. A thorough review of literature guided our choice of the most appropriate set of equations to describe the natural mass and energy exchange between a swimming pool and the environment. Monitoring of a pool in Davis, CA, was used to confirm the resulting simulations. Comparison of predicted and observed pool temperature for all hours over a 56 day experimental period shows an R-squared relatedness of 0.967.

© 2010 Elsevier Ltd. All rights reserved.

1. Introduction

In California, where all the large electric utilities experience their peak power demand in the summer, space cooling accounts for 29% of the total peak power demand and approximately 40% of the residential peak demand [1]. This occurs in part because the COP for traditional air-cooled vapor-compression cooling equipment diminishes significantly at high outdoor temperatures, such that equipment efficiency can be at its worst when cooling demand is greatest. Thermodynamics for heat pumps dictates that the work required to transfer heat from a cooler source to a warmer sink increases with the temperature difference between the two. In practice, for a vapor-compression system, since heat exchange with the refrigerant at the condenser and evaporator is driven by the temperature differences between the refrigerant and the sink and source respectively, the overall temperature difference experienced by the refrigerant is significantly larger than the temperature difference between the sink and source. For this reason, a large fraction of cooling efficiency research has focused on techniques to

reduce heat sink temperatures, and reduce the required temperature differences between the refrigerant and the source and sink. For example, rejecting condenser heat to water instead of air reduces the temperature difference that is needed for adequate heat transfer; air-cooled condensers typically require a refrigerant temperature that is 20 °C higher than condenser inlet air, while exchange with water only needs a 10 °C temperature difference.

The research presented in this paper provides a foundation for the design of cooling systems that reject condenser heat to swimming pools, a strategy that has been deployed successfully in many installations [2,3], but that has not been widely adopted. One reason for the lack of application is the lack of research, documentation and standardization. Our thesis is that a better understanding of the mechanisms that drive performance and savings could inform the development of guidelines for appropriate design of these systems, and could lead to more prevalent adoption, resulting in cost-effective energy and peak demand savings. The savings should come from three mechanisms:

1. Lower sink temperature since pool water is cooler than outdoor air during most cooling periods.
2. Improved heat transfer at the condenser since exchange with water is more effective than exchange with air.
3. Reduction of energy consumption for pool heating.

* Corresponding author. Tel.: +1 530 754 7670; fax: +1 530 754 7672.

E-mail addresses: jmwoolley@ucdavis.edu (J. Woolley), charrington@ucdavis.edu (C. Harrington), mpmodera@ucdavis.edu (M. Modera).¹ Tel.: +1 530 752 1101; fax: +1 530 754 7672.² Tel.: +1 530 754 7671; fax: +1 530 754 7672.

Nomenclature			
A_{cond}	surface area of conduction to ground (m ²)	p_a	ambient pressure (Pa)
A_s	surface area used for shape factor calculations (m ²)	p_o	reference pressure (Pa)
A	surface area of pool at air–water interface (m ²)	Pr	Prandtl number (–)
C_{Bowen}	Bowen coefficient ³ (61.3 Pa/°C)	\dot{q}_{ss}	dimensionless conduction heat rate (–)
d_{poolavg}	average pool depth (m)	q_{cond}	conduction heat flux (W/m ²)
e_a	vapor pressure in ambient air (Pa)	q_{conv}	convection heat flux (W/m ²)
e_s	saturation vapor pressure of air at the pool temperature (Pa)	q_{evap}	evaporation heat flux (W/m ²)
E_{sky}	emissivity of sky (–)	q_{rad}	radiation heat flux (W/m ²)
E_w	emissivity of water (–)	Q_{solar}	solar heat gain (W)
g	acceleration of gravity (m/s ²)	R_{Bowen}	Bowen ratio (–)
Gr_L	Grashof number (–)	Ra_L	Rayleigh number (–)
\bar{h}	average convection coefficient (W/m ² °C)	S	solar input (W/m ²)
h_{evap}	wind speed function for evaporation (W/m ² Pa)	T_a	ambient air temperature (°C)
HR	humidity ratio (kg/kg)	T_{dew}	dew point temperature (°C)
k_{air}	thermal conductivity of air (W/m °C)	T_w	swimming pool temperature (°C)
k_{soil}	thermal conductivity of soil (W/m °C)	T_{sky}	effective sky temperature (°C)
L	average length of pool (m)	T_{soil}	soil temperature (°C)
L_c	characteristic length of pool used for shape factor calculations (m)	V	wind speed (m/s)
\overline{Nu}_L	average Nusselt number (–)	α	absorptivity of water (–)
O_{sky}	opaque sky cover (tenths)	β_a	thermal expansion coefficient of air (1/°C)
P	perimeter of pool (m)	β_w	thermal expansion coefficient of water (1/°C)
		ρ	density of water (kg/m ³)
		σ	Stefan-Boltzmann constant (5.67 E ⁻⁸ W/m ² K ⁴)
		ν	kinematic viscosity of air (m ² /s)
		w	average width of pool (m)

The practical use of condenser heat rejection to swimming pools relies critically on the natural temperature regulation of pools by conductive heat exchange with the ground, convective and evaporative heat exchange with the air, and radiative heat exchange with the sky. The key is to balance heat rejection from the space cooling system with heating demand for the pool, such that pool temperature is maintained in a desirable range. We expect that this balance will be easiest to maintain in climate regions of the western United States, or other semi-arid regions with low ambient humidity and relatively low nighttime temperatures. In these regions, heat dissipation from swimming pools is increased by high evaporation rates in low humidity environments, and by longwave radiative cooling which increases with low ambient humidity and clear skies. Anecdotal evidence suggests that heat dissipation from pools in these climates is such that pool heating is often required to maintain desired water temperature, even when space cooling is required to maintain desired indoor temperature. In this case, heat rejected from cooling equipment could directly displace energy consumed to heat a pool, while concurrently improving the COP of the cooling system.

The objective of this paper is to document and discuss the development of a model to simulate the energy and mass balance of a swimming pool in natural interaction with its local environment; subsequent research will validate the model for simulation of a swimming pool used as a heat sink for vapor-compression air conditioning. Since there is no standardized approach to modeling the thermal behavior of swimming pools, this research draws from the conclusions of many authors to develop a clear and generalized method, and validates model predictions against long-term experimental measurements from a pool in Davis, CA.

³ The Bowen Coefficient is 6.13 Pa/°C for the case when evaporation from a water surface does not significantly impact absolute humidity of the air.

2. Methodology and results

2.1. Model development

An analytical model to determine the heat and mass transfer for a swimming pool was developed to calculate the transient thermal behavior of a pool based on hourly weather data. The model relies on detailed information about the site and the operating characteristics of the pool. Based on meteorological inputs and system conditions, at each hourly time step (t), the calculations draw on empirical and theoretical heat transfer correlations to estimate the steady state heat transfer rates for conductive, convective, radiative, and evaporative heat exchange mechanisms. Rates are integrated across the hour, and energy and mass storage terms are calculated to determine the average pool temperature at the beginning of the next hour ($t + 1$). Meteorological inputs and system conditions at ($t + 1$) are then used to solve for system conditions at the following hour ($t + 2$). The following sections describe the basis for calculating heat transfer rates for each mechanism considered in the model.

2.1.1. Insolation

The heat gain (W) due to solar radiation is found by multiplying the solar insolation at the pool surface by the absorptivity and area of the pool.

$$Q_{\text{solar}} = S \cdot \alpha \cdot A \quad (1)$$

The concept is simple, but determining the solar insolation and absorptivity are challenging prospects. Insolation at the pool surface is comprised of both direct and diffuse radiation, so when a pool is partly shaded by nearby objects, raw meteorological data for the global horizontal insolation is not representative of actual conditions. To compensate, shading of the pool must be described for each hour by inspection of the site and analysis of solar pathways for the latitude, season, and time period of the simulation. Diffuse insolation is used as the solar input for shaded periods and global

insolation is used for un-shaded periods; periods of fractional shading receive a corresponding fraction of global and diffuse insolation.

Absorptivity is even more complicated due to the phenomenon of multiplicative reflection and absorption in transparent materials. Only a portion of the solar radiation available at the pool surface is accumulated as heat in the water volume; a fraction is reflected by the water surface, and of the portion that passes unabsorbed through to the pool, a fraction is absorbed by the pool bottom and a fraction is reflected back into the pool. Water clarity affects the absorption rate per unit depth, and the pool construction, especially color, affects absorption at the pool bottom. Moreover, the fraction of radiation reflected from the water surface changes with solar incident angle, so the net absorptivity of the pool varies by time and season. However, for the model presented here, an annual average absorptivity was calculated using a method presented by Wu [4], which uses latitude, longitude, refractive index of water and air, pool bottom absorptivity, and average depth. The approach divides solar insolation into separate spectral bands to account for the fact that energy content and extinction rates vary as a function of wavelength; it considers multiplicative reflection and absorption, and the impact of incident angle. According to validation by Wu, the method predicts absorptivity to within 3.67% of experimental observations over the course of a day.

2.1.2. Conduction

Conduction between the swimming pool and ground is simpler to model, and in most circumstances accounts for less than 1% of the total energy loss from the pool [5–7]. Since the time constant of thermal response for the earth is very large, pool temperature only affects ground temperature very near the pool walls, and transient pool temperature has very little effect on the daily temperature distribution in the ground. Therefore, most authors assume that soil temperature remains constant, and since the temperature difference is small and conduction is minimal compared to other heat transfer mechanisms, many authors ignore this heat transfer component altogether. A review of the literature identified several different models to estimate conduction effects. All authors rely on a standard one-dimensional conduction equation; some use the thermal conductivity of the wall and a constant ground temperature, while others approximate a total thermal resistance for the pool wall plus soil in a temperature transition zone. Govaer [6] accounts for seasonal changes in ground temperature, but few account for the effect of a vertical temperature profile in the ground. Hull developed a semi-empirical method which uses the distance from the bottom of the pool to a constant temperature sink, the ground conductivity and pool dimensions [8]. The model presented here includes an analysis of conduction, but assumes a constant ground temperature, even across seasons, and a soil conductivity of 0.52 W/m-K [9].

While a three dimensional conduction model could be used, since the ground temperature is assumed to remain uniform and constant, this model simplifies the conduction problem to a one-dimensional function by using a shape factor to account for geometry effects. Shape factors have been developed analytically for many different geometric cases; for this model the swimming pool is approximated as a cuboid embedded in an infinite medium, and a shape factor given by Incropera [9] is adapted to account for heat transfer through five faces of the cuboid with ground interface area similar to that of the pool.

d/D	\dot{q}_{ss}
0.1	0.943
1.0	0.956
2.0	0.961

$$q_{\text{cond}} = \frac{1}{2L_c} \dot{q}_{ss} k_{\text{soil}} \frac{A_s}{A_{\text{cond}}} (T_{\text{soil}} - T_{\text{pool}}) \quad (2)$$

where

$$A_s = 2D^2 + 4Dd \quad (3)$$

$$d = 2d_{\text{poolavg}} \quad (4)$$

$$L_c = \left(\frac{A_s}{4\pi} \right)^{0.5} \quad (5)$$

$$D = \left(A_{\text{cond}} + d^2 \right)^{0.5} - d \quad (6)$$

2.1.3. Radiation

Exchange of longwave radiation with the sky is one of the most significant pool cooling effects; it occurs continuously, separate from solar radiation. The magnitude of this heat flux is calculated using equation (7), the standard radiative heat transfer equation. The approach relies on the effective sky temperature – a value that reduces the complex phenomenon of radiant exchange between the pool, the semi-opaque atmosphere, and space beyond, to a simple radiative exchange between the pool and a much larger surface of representative temperature. Walton [10] developed two methods to determine the effective sky temperature; one is a function of infrared radiation from the sky, the other relies on the dew point temperature, sky emissivity and opaque sky cover. The latter approach was used here, as the infrared sky radiation is not generally measured by standard meteorological stations.

$$q_{\text{rad}} = \sigma E_w \left[(T_{\text{sky}} + 273)^4 - (T_w + 273)^4 \right] \quad (7)$$

$$T_{\text{sky}} = (T_a + 273) \cdot \left(E_{\text{sky}}^{0.25} \right) - 273 \quad (8)$$

$$E_{\text{sky}} = \left[0.787 + 0.764 \cdot \log \left(\frac{T_{\text{dew}} + 273}{273} \right) \right] \left[1 + 0.224 \cdot O_{\text{sky}} - 0.0035 \cdot O_{\text{sky}}^2 + 0.00028 \cdot O_{\text{sky}}^3 \right] \quad (9)$$

This radiative heat transfer decreases with increases in dew point temperature, opaque sky cover, and ambient air temperature. It can account for up to 60% of the total thermal losses at night in arid climates with low humidity, minimal cloud cover, and low nighttime temperatures. Compared with the other two parameters, dew point temperature, an indicator of ambient humidity, has a relatively small impact on the overall longwave radiative heat transfer. However, there is an obvious correlation between low ambient humidity and a low degree of cloud cover. Fig. 1 and Fig. 2 illustrate the magnitude of longwave radiation loss (W/m²) as a function of opaque sky cover and ambient temperature respectively. Note that heat flux into the pool is the positive convention, so negative exchange of longwave radiation represents cooling of the pool. It is critical for the model's accuracy to obtain cloud cover data for each hour of the day because, as Fig. 1 shows, the radiative heat transfer can differ significantly between clear sky and cloudy conditions.

2.1.4. Evaporation

Evaporation is an especially complicated phenomenon to model for swimming pools since:

1. There is no commonly accepted theoretical approach for estimating evaporation rates from free water surfaces [11]
2. Empirical equations may only be appropriate under the conditions for which they were developed

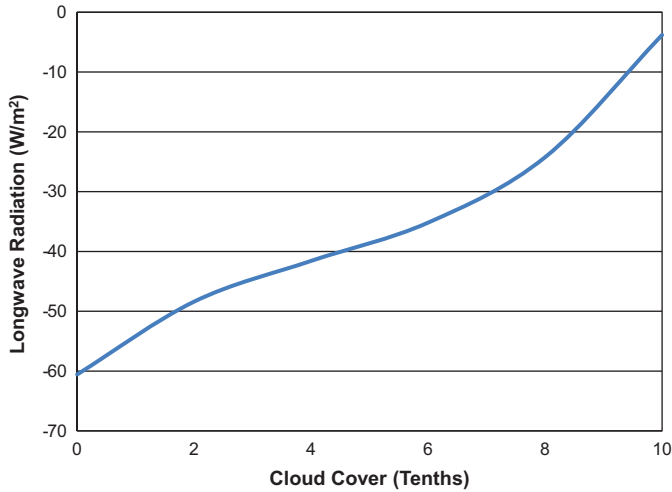


Fig. 1. Exchange of longwave radiation as a function of cloud cover ($T_a = 30\text{ }^\circ\text{C}$, $HR = 0.010$, $T_w = 25\text{ }^\circ\text{C}$).

3. Evaporation is sensitive to local environmental conditions, which differ from available meteorological data due to the proximity of obstructions such as buildings and trees, and microclimatic patterns related to neighborhood scale phenomena

The model developed herein couples empirical formulae for mass transfer from free water surface evaporation with empirical and theoretical heat transfer correlations to develop a more complete model of the evaporative heat and mass transfer mechanisms at play in a swimming pool.

Evaporation is driven by wind speed, and by the difference between the saturated vapor pressure of air at the pool surface temperature and the vapor pressure of ambient air. Thus, evaporation is greater in arid climates, and is typically the most significant heat transfer mechanism for the overall energy balance of a pool. Equations (10) and (11) were developed by McMillan [12], and confirmed by Sweers [13] and Sartori [11]. They describe the relationship between evaporative heat transfer and relevant environmental conditions.

$$q_{\text{evap}} = -h_{\text{evap}} \cdot (e_s - e_a) \tag{10}$$

$$h_{\text{evap}} = 0.0360 + 0.0250 \cdot V \tag{11}$$

where the wind velocity V is corrected to a height of 3 m.

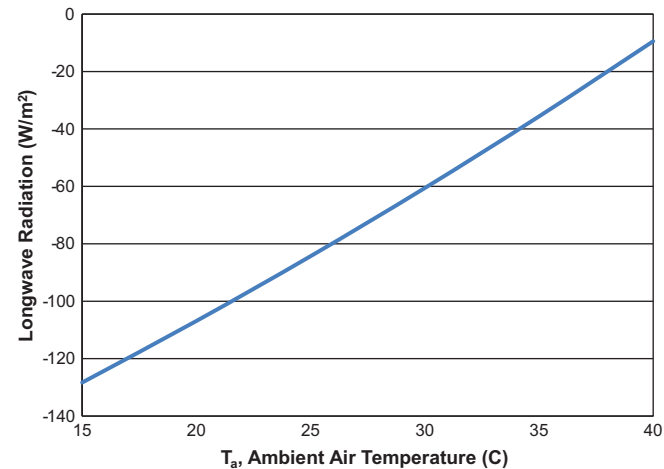


Fig. 2. Exchange of longwave radiation as a function of ambient air temperature (clear sky, $HR = 0.010$, $T_w = 25\text{ }^\circ\text{C}$).

These equations were developed experimentally by correlating water temperature in several lakes to meteorological measurements of air temperature, relative humidity, and wind speed. A negative value for q_{evap} indicates that water is evaporated, sensible heat is lost from the water mass, and latent heat is gained in the air mass. The empirical wind speed function for evaporation, h_{evap} , accounts for the latent energy content of water vapor and the rate at which water vapor diffusion occurs under different wind conditions, while the equation for q_{evap} accounts for the evaporative potential due to the difference between vapor pressure in the ambient air and saturation conditions at the water surface temperature. It's worth noting that the evaporation rate is driven by the relationship between pool temperature and the absolute humidity of the ambient air, but it is not directly correlated to the ambient dry bulb temperature.

2.1.5. Convection

Evaporative and convective heat transfer phenomena are related; they operate by very similar mechanisms and can be reasonably conceptualized as a single process of coupled heat and mass transfer. Mass transfer and the associated transformation of sensible heat to latent heat occur by evaporation, while sensible heat transfer occurs by convection. A difference in absolute humidity, or vapor pressure, is the driving potential for evaporation, and a temperature difference is the driving potential for convection. Wind affects both by increasing the total effective interface for heat and mass transfer, and notwithstanding the role of wind, evaporation and convection are rate limited by mass diffusivity and thermal diffusivity respectively. The evaporation equations indicate that the water mass provides all sensible heat for phase change to latent heat through evaporation. However, if you consider evaporation and convection together, it is clear that as the water cools sensibly due to evaporation, convective heat transfer rates will shift, and given that the air is warmer than the water surface some sensible heat for evaporation will effectively be drawn from the air by convection. In contrast, if evaporation occurs under conditions where the air is cooler than the water, all sensible heat for evaporation must necessarily be derived from the water mass. Thus, as the two phenomena are closely related, the convective heat transfer rate can be derived theoretically as a function of the evaporative heat transfer rate. Bowen [14] expresses the relationship as a ratio:

$$\frac{q_{\text{conv}}}{q_{\text{evap}}} = R_{\text{bowen}} \tag{12}$$

which can be calculated by:

$$R_{\text{bowen}} = C_{\text{Bowen}} \cdot \frac{p_a}{p_o} \cdot \frac{(T_w - T_a)}{(e_s - e_a)} \tag{13}$$

Bowen developed this formula from first principles, based on a control volume analysis of sensible and latent heat densities in a differentially small element of air, subject to molecular and thermal diffusivity, and forced air movement. Note that the formula accounts for the impact of ambient pressure on the ratio of convective and evaporative heat transfer. Using the Bowen ratio, the convective heat transfer rate is determined simply by multiplying by the evaporative heat transfer rate:

$$q_{\text{conv}} = R_{\text{bowen}} \cdot q_{\text{evap}} \tag{14}$$

The net heat transfer by the coupled process of convection and evaporation is simply the sum of q_{conv} and q_{evap} . Fig. 3 plots R_{bowen} alongside the net heat transfer by convection plus evaporation, for several different ambient dry bulb temperature conditions, all as a function of humidity ratio. Note that the humidity ratio at low

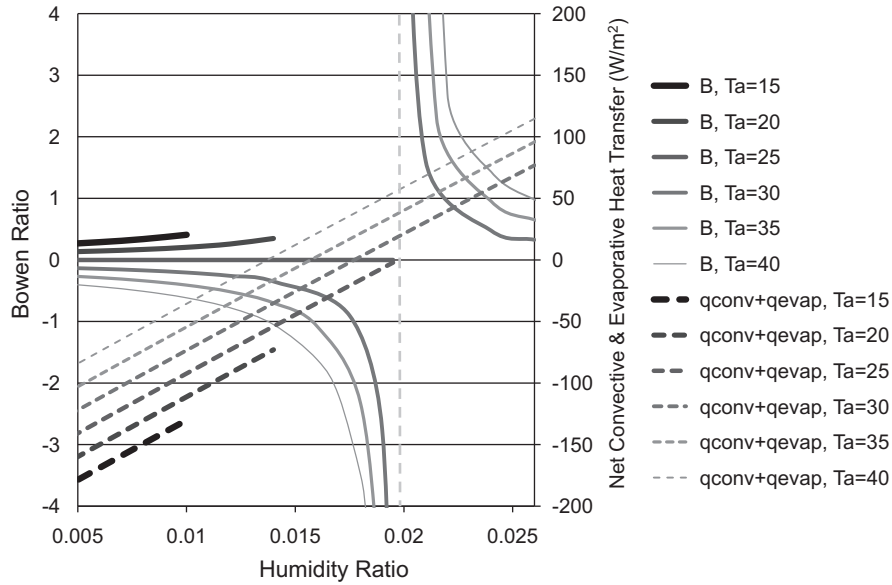


Fig. 3. Plot of Bowen ratio and net heat transfer by convection and evaporation, for several different ambient dry bulb temperatures, as a function of humidity ratio. Wind speed = 1 m/s, water temperature = 25 °C.

ambient dry bulb temperatures is limited by saturation, and that the Bowen ratio diverges asymptotically at the saturation humidity for air at the water surface temperature.

For conditions where humidity of the ambient air is less than the saturation humidity at the water surface temperature (the left side of Fig. 3), a positive Bowen ratio indicates that heat is lost from the water mass by both evaporation and convection. As illustrated by the net convective and evaporative heat transfer lines in Fig. 3, these conditions result in the maximum water cooling effect. As ambient dry bulb temperature approaches the water surface temperature the Bowen ratio approaches zero. At this point no heat is exchanged by convection, though heat may still be lost from the water by evaporation. A negative Bowen ratio indicates that evaporation and convection have opposing effects. A ratio between 0 and -1 means that the cooling effect of evaporation is dominant, a ratio of -1 indicates a net-zero balance of convection and evaporation, and a ratio beyond -1 means that convective heat gains to the pool dominate evaporative losses, resulting in a net heat gain to the water. For conditions where ambient humidity is greater than the saturation humidity at the water surface temperature (the right side of Fig. 3), condensation and convection will both contribute heat to the water mass. Note that for such conditions the Bowen ratio must be positive, since such absolute humidity conditions cannot occur for air temperatures below the water surface temperature.

At zero wind speed, the solution of equation (14) should equate to other well developed theoretical models for heat transfer. When the water surface temperature is greater than the air temperature the solution should agree with models for buoyancy driven free convection. If water surface temperature is less than the air temperature, air movement should stagnate above the water mass and equation (14) should yield similar results to models for conduction with a semi-infinite non-circulating mass. Equations (15) through (18), presented by Incropera [9], were used to validate equation 14 at zero wind speed for cases of buoyancy driven free convection; equations (19) through (21) were used similarly for conduction with a stagnant air mass.

For buoyancy driven convection:

$$q_{\text{conv}} = \bar{h} \cdot (T_w - T_a) \quad (15)$$

where:

$$\bar{h} = \frac{\overline{Nu}_L \cdot k_{\text{air}}}{L_c} \quad (16)$$

$$L_c \equiv \frac{A}{P} \quad (17)$$

$$\overline{Nu}_L = Ra_L^{1/3} \quad (10^7 \leq Ra_L \leq 10^{11}) \quad (18)$$

and for conduction with non-circulating air:

$$q_{\text{conv}} = 0.932 \cdot \frac{k_a(T_w - T_a)}{L_c} \quad (19)$$

where:

$$L_c = \sqrt{\frac{A_s}{4\pi}} \quad (20)$$

$$A_s = 2wL \quad (21)$$

The result of this validation shows that at zero wind speed, deriving the average convective heat transfer rate from the evaporative heat transfer rate and the Bowen Ratio, as described by equation (10), agrees with other well developed models for buoyancy driven convection or conduction in a non-circulating air mass to within 5%.

2.1.6. Other mechanisms

Other mechanisms that affect the pool temperature include swimmers, rain, makeup water, pool covers, and the thermal effect of pumps. Accounting for swimmers is particularly difficult because of the myriad variables involved, though some authors have considered it. For example, Molineaux [15] assumes a heat addition of approximately 400 calories per swimmer per hour, which would have a measurable effect on water temperature in a pool with heavy use. The impacts of rain and makeup water may be significant in certain instances and can be calculated by accounting for the mass and temperature of the added water, though these values may be difficult to estimate. Pool covers can significantly impact the thermodynamics of a pool, mostly by eliminating evaporation and reducing longwave radiative losses. Each pool

cover has different absorptive, emissive, and insulative properties and must be modeled accordingly. Pumps contribute heat to the pool, in part through frictional interactions with piping and dissipation of kinetic energy, and in part by way of heat generated within the pump. The design, operation, and site-specific meteorological characteristics of each pool will impact the relative importance of each of these heat additions, such that in certain cases they should be included in the model.

2.2. Model validation

To validate the calculations discussed herein, an experiment was conducted at a residential swimming pool in Davis, CA, a relatively hot and dry region in California Climate Zone 12. The thermal behavior of the pool was monitored over a 56 day period in spring 2009, and observations were compared to results from the model using hourly meteorological data for the same time period. The pool was left uncovered, no swimmers were permitted, no makeup water was added, and the filter pump was set to run continuously at a constant flow rate (Fig. 4).

2.2.1. Methodology for experimental validation

The model requires definition of an initial pool temperature, as well as several meteorological variables on an hourly basis, including: global horizontal insolation, pool shading, cloud cover, ambient dry bulb temperature, ambient humidity, wind speed, and barometric pressure. Future iterations of the model will accept the definition of an hourly thermal input from vapor-compression cooling equipment, though this study focuses on validation of the thermodynamic balance between a passive swimming pool and the environment.

Note that an accurate initial pool temperature is not absolutely necessary for the model to appropriately predict the long-term hourly temperature behavior of the pool, though it may take up to a few weeks for the model to track the actual pool temperature if the initial conditions are off by 5 °C. The results presented here use measured pool temperature as an initial condition for the simulation.

Although global horizontal solar insolation could be measured on site, in certain instances it is impossible to install a pyranometer in a completely un-shaded location; thus the model is designed to allow input from offsite meteorological measurements. The global horizontal insolation for each hour of the experiment was obtained

from the California Department of Water Resources' California Irrigation Management Information System (CIMIS) [16] which reports measurements for a meteorological station in Davis, CA, as well as hundreds of other sites throughout the state. The meteorological station used to obtain hourly insolation values was close by and assumed to be representative of the test site. The direct and diffuse portions of this measurement were calculated using a quasi-physical model for converting hourly global horizontal to direct normal insolation developed by Maxwell and published by the NREL Solar Energy Research Institute [17].

Since the meteorological measurements of insolation are fully exposed, whereas pools are often surrounded by obstructions, an hourly shading factor for the pool was developed by inspection of the site and an analysis of solar pathways for the latitude, season, and time period of the experiment. The model uses diffuse insolation as the solar input for shaded periods and global insolation for un-shaded periods; periods of fractional shading receive a corresponding fraction of global and diffuse insolation.

For the experimental validation presented here, ambient temperature, relative humidity, and wind speed were measured on site. Some error is incurred due to slight variations in meteorological conditions at different points on site; however, the location of each measurement was selected to avoid significant misrepresentation of conditions at the pool surface. For example, the anemometer was placed to avoid eddies and vortices that could occur very near a building. The wind speed measurement was corrected to a 3 m height using standard atmospheric boundary layer methods [18] since the McMillan wind speed coefficient presented in equation (11) is derived for wind speed at that height. These measurements could all be taken from regional meteorological data, or from typical meteorological year resources, though microclimatic variations between a meteorological station and an actual site introduces errors that are not associated with the mathematical model itself. Wind speed is an especially sensitive input variable. Since meteorological stations tend to be located in open, unobstructed areas, and sites of interest are often surrounded by nearby obstructions such as trees, fences, and buildings, measurements near to the ground do to not scale well using standard atmospheric boundary layer methods to correct for terrain differences. For example, over the test period presented here, CIMIS wind speed observations at 2 m in open terrain and corrected to 3 m in a highly obstructed urban area were consistently high as

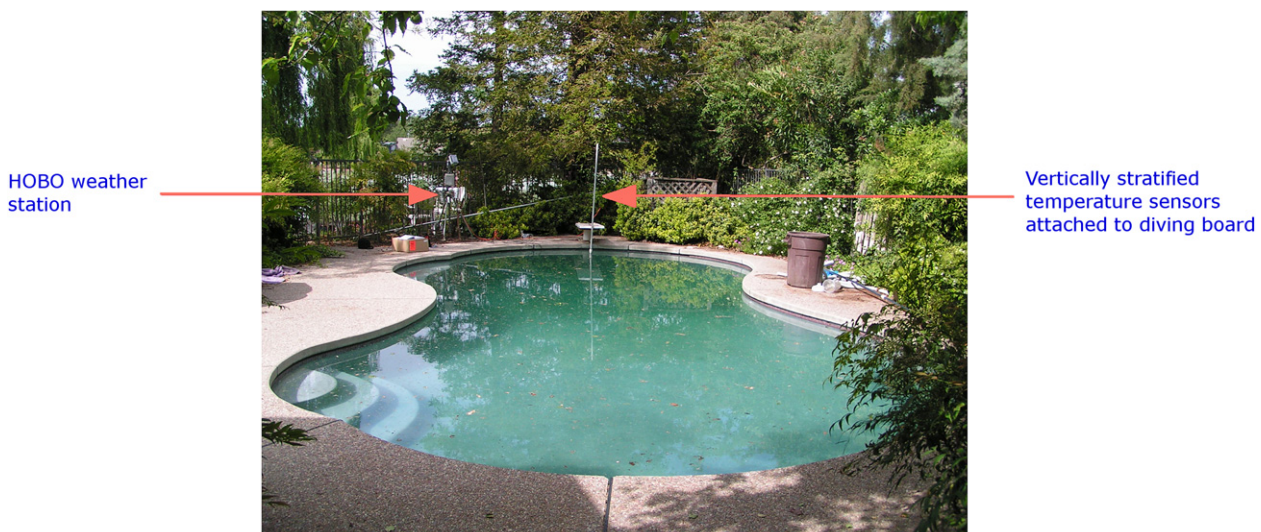


Fig. 4. Photo of pool in Davis California used for experimental validation.

compared to actual measurements, with an RMS error of 1.6 m/s. This overestimation of wind speed would result in a consistent under estimation of pool temperature. Relative humidity and ambient temperature measurements vary as well, such that the pool temperature predictions from a simulation using CIMIS data and a simulation using site data differ with an RMS error of 3.0 °C.

Calculation of longwave radiative exchange requires information about the fractional portion of the sky dome that is obstructed by clouds, though this data is not regularly collected by all meteorological stations. For this simulation, data was obtained from the National Oceanic and Atmospheric Administration's (NOAA) Quality Controlled Local Climatological Database (QCLCD) [19] for a station in Sacramento, CA, which is about 20 miles from the experimental site.

Conduction between the pool and earth was calculated using a constant soil temperature of 15 °C. Transient effects due to diurnal and seasonal heat transfer from the pool were ignored, and the pool geometry was approximated as a cuboid as described previously by equation (6).

The temperature of the pool was measured at 1', 4', and 7' from the pool bottom to develop an average pool temperature and to describe the extent of thermal stratification. For this experiment, since the filter pump ran continuously at a constant flow rate, the pool was relatively well mixed and no thermal stratification was observed.

2.2.2. Validation results

The model described herein used the initial inputs and hourly meteorological conditions to determine heat and mass exchange between the pool and environment, and to predict hourly average pool temperature. The predicted values were then compared to the observed temperature history and analyzed for accuracy, Fig. 5 illustrates the results.

The results suggest that, given input of appropriate meteorological conditions, an accurate prediction of the pool temperature can be made. The RMS error of the pool temperature prediction compared to measured values is 0.4 °C and the largest discrepancy is only 1.1 °C. The temperature sensors used in the experiment had an absolute error of ± 0.2 °C, so accuracy of the model is very near sensor accuracy.

The most significant periods of error between measured and predicted pool temperature occur for approximately one week near the beginning of the test period, and for several days near the middle of the test period. The first instance is likely due to a storm that brought cloud cover and measurable precipitation. Although the model responds to data for both opaque cloud cover and global

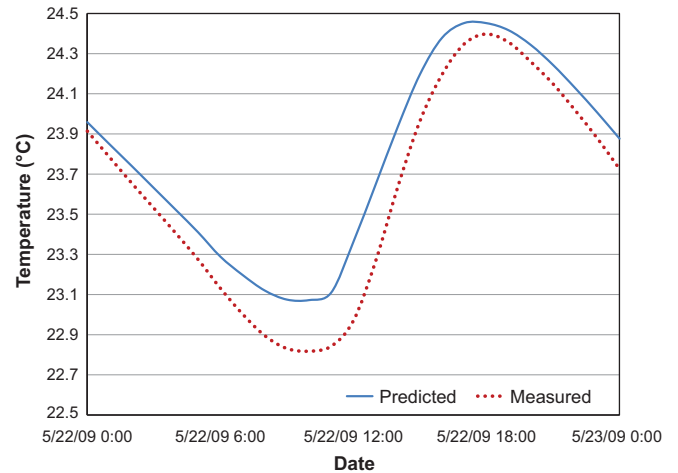


Fig. 6. Predicted and measured temperatures for a case of very good accuracy.

horizontal insolation, since those values were measured at offsite meteorological stations they could differ somewhat from local conditions. The error during this period can be reduced almost completely if values for cloud cover are inflated, but there are no theoretical grounds to include such adjustments in the model. The periods of error in the middle of the test are not related to any obvious meteorological event, and are not easily explained. In all instances the discrepancy rarely reaches 1.0 °C. It is noteworthy that the model recovered from poor prediction periods automatically, without any input other than the new meteorological data, which suggests that it is a robust model.

Figs. 6 and 7 illustrate typical diurnal cycles for the pool during the observed period. Fig. 6 is an example of one day for which the model gives a very accurate prediction, while Fig. 7 is for a relatively poor prediction. In both instances the simulation is in phase with the measurements; though the measured pool temperature transitions gradually between heating and cooling, while the predicted pool temperature responds more abruptly. This is likely due to the hourly time step implemented in the simulation. In a physical system meteorological conditions change continuously while the model relies on constant values for each hour. If weather data were resolved more continuously the model would respond more gradually.

Fig. 8 plots all hourly predicted pool temperatures against all hourly measured pool temperatures. A perfectly accurate model

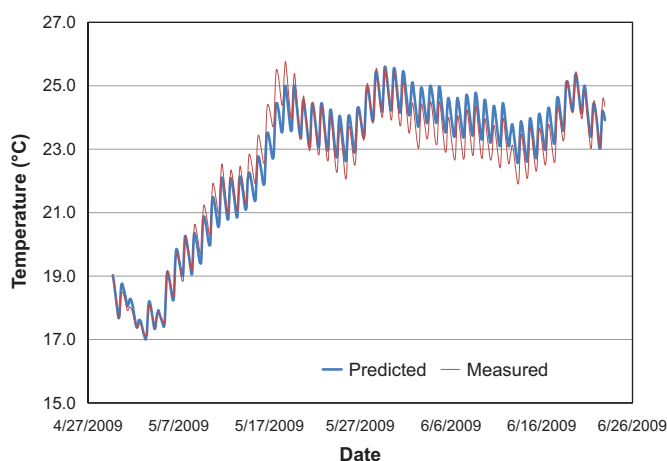


Fig. 5. Predicted and measured pool temperatures for a pool in Davis California observed 4/29/2009–6/22/2009.

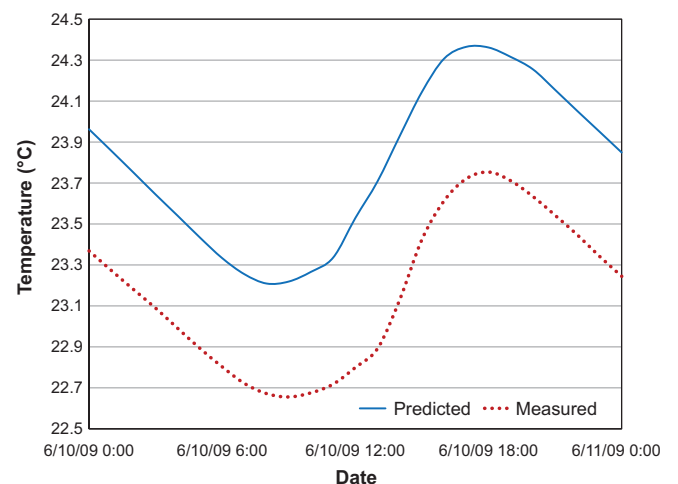


Fig. 7. Predicted and measured temperatures for a case of poor accuracy (error of 0.6°).

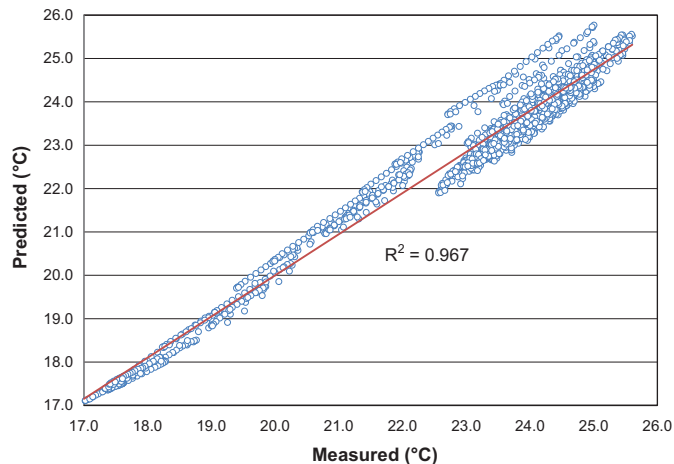


Fig. 8. Comparison of predicted and measured pool temperature for all hourly observations.

would have a one-to-one relationship between the values. For the period of validation this simulation has very good fit with an R^2 value of 0.967.

The relative impact of each heat transfer mechanism over the duration of the experiment is illustrated in Fig. 9. Note that solar insolation is the only heat gain, the sum of all heat losses balances with the solar gains, and that evaporation and emission of longwave radiation dominate over conduction and convection.

Fig. 10 plots the magnitude of each heat transfer mechanism and the total heat accumulated across two typical days from the experiment. Convection and longwave radiative exchange with the sky are affected directly by diurnal air–temperature cycles while evaporation is not. Note that heat flux into the pool is the positive convention, so negative values represent cooling of the pool. Longwave radiative exchange with the sky is consistently negative since the effective sky temperature never exceeds the pool temperature during the plotted period.

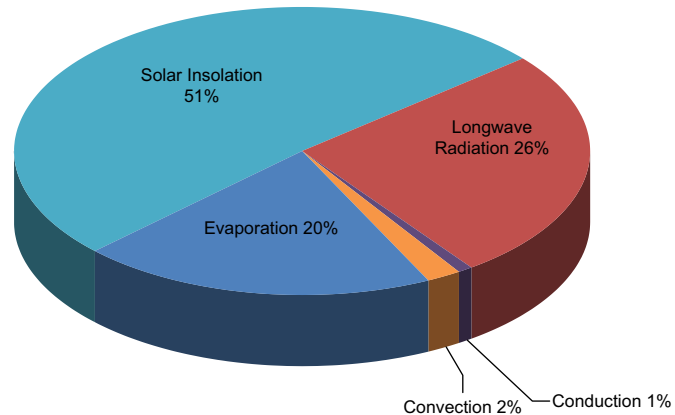


Fig. 9. Relative magnitude of each heat transfer mechanism integrated across the duration of the experiment.

3. Discussion

3.1. Experimental considerations

Although average pool temperature has been presented as the metric by which to validate simulations, mass evaporation could be used as well. The predicted mass evaporation rate can be calculated directly in the model by relating heat transfer by evaporation to the latent heat of vaporization of water; and the actual cumulative evaporation can be measured directly by monitoring the water level. However, since the mass rate of evaporation is small compared to pool volume, it is very difficult to accurately measure changes in depth on an hourly basis. The barometrically corrected water depth sensors used for our experimentation are accurate to within 0.0035 m, so for a pool with 50 m² surface area and 5 kg/h evaporation the hourly change in depth of 0.0001 m cannot be reliably observed, especially considering the noise associated with naturally occurring disturbances to the water surface. The issue was further complicated in this experimental validation because the

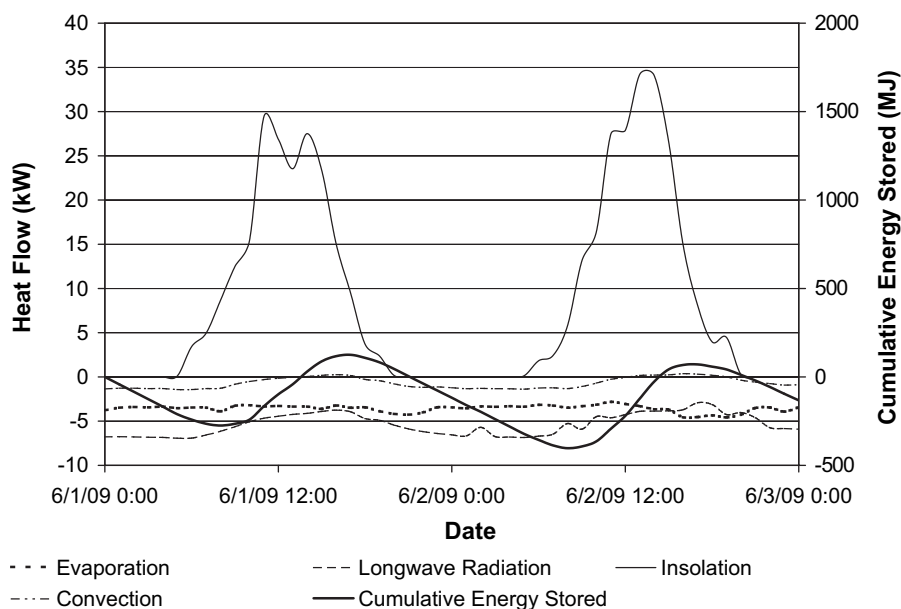


Fig. 10. The magnitude of each heat transfer mechanism and heat accumulation for two typical days of the experiment (conduction heat flow was omitted from this figure as it was effectively zero).

depth sensor was mounted to a pole at the end of a diving board, which seemed to expand and contracted slightly with diurnal temperature cycles, causing sensor movement and misrepresentation of fluctuations in water depth. In subsequent field tests the depth sensor will be placed at a fixed point, and the water column above the sensor will be isolated from small disturbances to the pool surface.

3.2. Future work

The next phase of model development and validation involves the addition of heat from vapor-compression space cooling equipment, and the development of design guidelines for such heat pump systems in various climate zones in the western United States. A preliminary simulation was conducted for the pool studied here with the addition of heat rejected from a condenser. The condenser heat for each hour was calculated for a 3.5 ton heat pump assuming a constant COP, and was based on cooling loads generated in MICROPAS [20] for a 1764 square foot, single story home in California Climate Zone 12. Under this scenario the pool temperature never exceeded 28.5 °C. Another experiment will be conducted to compare this model with observations from a geothermal heat pump system that is coupled to a swimming pool with a gas-fired pool heater, solar thermal pool heaters, night radiative coolers, and fountains for evaporative water cooling. The intent is to account for the impact of all system components in the model in order to simulate performance under various configurations in multiple climate zones and develop guidelines to reduce energy consumption for space cooling while preventing overheating. Additionally, future work will explore the potential to offset pool heating costs during swing seasons when pool temperatures are low yet space cooling is required. Research is needed to clarify when this occurs and how much energy could be saved in various climate zones, and with different degrees of pool shading.

4. Conclusions

Predictions from the mathematical model developed match well with measured pool temperature results, suggesting that it could be used to accurately analyze the temperature response of a pool used as a thermal sink for a heat pump during the cooling season, or as a thermal source for a heat pump in the heating season. The accuracy of the model is impressive, and is due mostly to the extensive theoretical and empirical research by other authors to explain each heat transfer mechanisms at play in this scenario. It should be noted that our methodology to describe shading of the pool each hour is the only variable that was not derived from other published work or directly measured with instrumentation, and that no “correction factors” have been used to calibrate the model against the measurements. Although the model is very accurate, if used as a design tool it should be noted that meteorological conditions at a site may differ significantly from available data, and that predictions may not be as accurate as the validation results presented here. The test period allowed for validation of the model

under multiple environmental conditions including clear and cloudy scenarios, as well as cool and very hot conditions. However, the model was not validated for extended cold periods, heavy rain conditions, mechanical thermal loading, or extreme climates.

5. Legal notice

This report was prepared as a result of work sponsored by the California Energy Commission (Energy Commission) and the University of California (UC). It does not necessarily represent the views of the Energy Commission, UC, their employees, or the State of California. The Energy Commission, the State of California, its employees, and UC make no warranty, express or implied, and assume no legal liability for the information in this report; nor does any party represent that the use of this information will not infringe upon privately owned rights. This report has not been approved or disapproved by the Energy Commission or UC, nor has the Energy Commission or UC passed upon the accuracy or adequacy of the information in this report.

References

- [1] Brown EG. In: Justice DO, editor. Framework document for central air conditioners and heat pumps; 2008. Oakland.
- [2] Turpin JR. Homeowners dive into savings. In: Air conditioning, heating & refrigeration news; 2009.
- [3] Randazzo R. Shasta pools develops unique cooling system. Phoenix: The Arizona Republic; 2009.
- [4] Wu H. A mathematical procedure to estimate solar absorptance of shallow water ponds. Energy Conversion and Management 2009;50:1828–33.
- [5] Hahne E. Monitoring and simulation of the thermal performance of solar heated outdoor swimming pools. Solar Energy 1994;53(1):9–19.
- [6] Govaer D. Analytical evaluation of direct solar heating of swimming pools. Solar Energy 1981;27:529–33.
- [7] Rakopoulos CD. A model of the energy fluxes in a solar heated swimming pool and its experimental validation. Energy Conversion Management 1987;27(2):189–95.
- [8] Hull JR. Dependence of ground heat loss upon solar pond size and Perimeter insulation – calculated and experimental results. Solar Energy 1984;33(1):25–33.
- [9] Incropera. Introduction to heat transfer. 5th ed. Wiley; 2007.
- [10] Walton G. Thermal analysis research program reference manual. National Bureau of Standards, NBSIR; 1983. p. 83–2655.
- [11] Sartori E. A critical review on equations employed for the calculation of the evaporation rate from free water surfaces. Solar Energy 1999;68:77–89.
- [12] McMillan W. Heat dispersal – lake Trawsfynydd cooling studies. Symposium on Freshwater Biology and Electrical Power Generation 1971;1:41–80.
- [13] Sweers HE. A nomogram to estimate the heat-exchange coefficient at the air–water interface as a function of wind speed and temperature; a critical survey of some literature. Journal of Hydrology 1976;30:375–401.
- [14] Bowen IS. The ratio of heat losses by conduction and by evaporation from any water surface. Physical Review 1926;27:779–87.
- [15] Molineaux B. Thermal analysis of five outdoor swimming pools heated by unglazed solar collectors. Solar Energy 1994;53(1):21–6.
- [16] California Irrigation Management Information System. California Department of Water Resources, Office of Water Use Efficiency; 2009.
- [17] Maxwell EL. A quasi-physical model for converting hourly global horizontal to direct normal insolation. Midwest Research Institute; 1987.
- [18] ASHRAE handbook, fundamentals. 2009 ed. American Society of Heating, Refrigeration, and Air-Conditioning Engineers, Inc; 2009.
- [19] Quality Controlled Climatological Database, US Department of Commerce, National Oceanic and Atmospheric Administration, National Environmental Satellite, Data, and Information Service, National Climatic Data Center.
- [20] MICROPAS; 2010.